Electron. Mater. Lett., Vol. 13, No. 4 (2017), pp. 330-338
DOI: 10.1007/s13391-017-6231-5

Swift Heavy Ion Induced Modifications in Optical and Electrical Properties of Cadmium Selenide Thin Films

Ritika Choudhary and Rishi Pal Chauhan*

Department of Physics, National Institute of Technology, Kurukshetra, Haryana 136119, India

(received date: 20 July 2016 / accepted date: 10 February 2017 / published date: 10 July 2017)

The modification in various properties of thin films using high energetic ion beam is an exciting area of basic and applied research in semiconductors. In the present investigations, cadmium selenide (CdSe) thin films were deposited on ITO substrate using electrodeposition technique. To study the swift heavy ion (SHI) induced effects, the deposited thin films were irradiated with 120 MeV heavy Ag^{9+} ions using pelletron accelerator facility at IUAC, New Delhi, India. Structural phase transformation in CdSe thin film from metastable cubic phase to stable hexagonal phase was observed after irradiation leading to decrease in the band gap from 2.47 eV to 2.12 eV. The phase transformation was analyzed through X-ray diffraction patterns. During SHI irradiation, Generation of high temperature and pressure by thermal spike along the trajectory of incident ions in the thin films might be responsible for modification in the properties of thin films.

Keywords: thin films, heavy ion irradiation, X-ray diffraction, electrical properties, optical properties

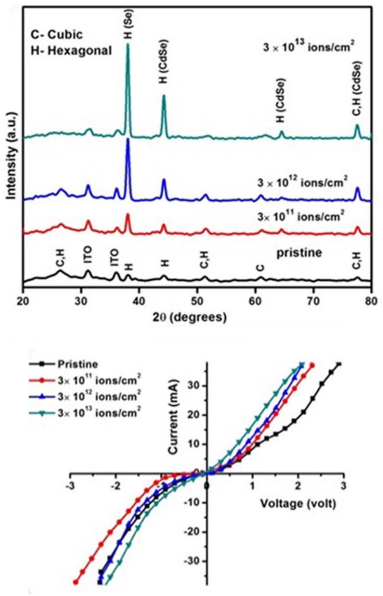

1. INTRODUCTION

CdSe is a wide and direct band gap semiconductor belonging to II-VI group of semiconductors.[1] Selenium based semiconductors have many disadvantages like short life time and low photosensitivity. To overcome these disadvantages, different combination of materials may be used. The adding of group II materials to Se (VI) has developed considerable interest because of their wide potential applications in thermoelectric, optoelectronics, and memory based devices.[2-4] Thin films of CdSe have better carrier mobility as compared to Si films and can be used in solar cells as an absorber layer.[5,6] Various techniques like physical vapor deposition,[7] thermal evaporation,[8] chemical vapor deposition,[9] dip coating,[10] sputtering,[11] and electro-deposition[12] etc. have been used for depositing thin films. But among them electro deposition is one of the simplest and low-cost technique for the deposition of thin films as compared to others. In this technique, the deposition rate can be easily controlled by changing various parameters like applied voltage, time of deposition, pH of the electrolyte, solution concentration etc.[13,14]

Modification in the properties of thin films by swift heavy ion (SHI) irradiation, γ-rays and high energy particles (electron, proton) has gained much attention in recent years. The irradiation of materials with high energetic ions leads to the creation of a wide variety of defects within the materials. These defects may generate energy levels in the band gap which alters the structural, electrical transport and optical

*Corresponding author: chauhanrpc@gmail.com

properties of the materials. These effects of irradiation strongly depend upon energy, mass and fluence of the incident ion. The irradiation may cause ionization or excitation and hence possibly lead to the displacement of atoms from their lattice sites in the materials. SHI is very useful for the modification in the properties of the thin films, foil and surface of bulk solids. The high energetic ions penetrate deep into the materials and produce a long and narrow disorder zone along their path. When a swift heavy ion penetrates into a solid, it is slowed down via two processes: (i) direct transfer of energy to target atoms through elastic collisions (Nuclear Energy Loss, S_n) and (ii) electronic excitation and ionization of target atoms through inelastic collisions (Electronic Energy Loss, S_e). The S_n induced process dominates where ions possess energies in the range of 10-100 keV and leads to the creation of atomic size point-defects and cluster of defects. The S_e induced process dominates in the higher energy region (10-100 MeV), where the velocity of the incident ion is comparable to Bohr velocity of the valence electrons. The incident ions make inelastic collisions with the atoms of the material and the atoms get excited or ionized. If the thickness of the target is sufficiently smaller than the range of the projectile ions, then the energy deposition is mainly due to electronic energy loss. This energy deposition leads to the production of defects and heat in the material thereby resulting in the processes like crystallization, amorphization and phase transformation in the target material.[15-17] Swift heavy ion (SHI) irradiation is a unique tool offering several possibilities to synthesize or modify the materials in a controlled way with great precision (through ion dose), spatial selectivity (either by focusing or by using high energies) and depth (through energy). A variety of structural modifications such as structural phase transition, creation of point defects, defect clusters, crystallization, and amorphization may appear during irradiation using SHI owing to the electronic excitation within a narrow disorder zone.[18-20] In order to explain the SHI induced structural phase transformation in nanocrystalline thin film, it is necessary to understand the interaction process of SHI with materials. As the electronic energy loss (S_e) process dominates at higher ion energies, so the modification is expected only due to the energy transferred to electrons of the target system during passage of the energetic ions. There are two models which explain the effect of electronic energy loss in materials viz. coulomb explosion model and thermal spike model.[17,21,22] SHI irradiation leads to the formation of cylindrical zone of dense electronic excitation/ionization along the ion trajectory.[23] During electronic excitation, ions transfer most of their energy to the electronic system of target and then to the lattice via electron-phonon interactions. This transferred energy is so high that the lattice system melts within a fraction of a second (10^{-12} s), known as thermal spike. It may happen that with high temperature occurring during thermal spike, generation of high pressure, known as pressure spike also takes place.[21,24] Generation of high temperature and pressure during MeV ion irradiation along the ion trajectory in the films is responsible for the structural phase transformation. There are only a few reports in the literature which explains the structural phase transformation in thin films by SHI irradiation. The structural phase transformation from wurtzite (W) hexagonal phase to zinc-blende (ZB) cubic phase observed in ZnS nanocrystalline thin films by swift heavy Ni ion (150 MeV) irradiation.[25] 100 MeV Ag ions induced structural changes from metastable cubic to hexagonal phase in CdS thin film and metastable hexagonal phase to stable cubic phase in CdTe thin film was also reported.[18,19] In the present work, the effects of Swift heavy Ag^{9+} ion of energy 120 MeV on the CdSe thin film of thickness 110 nm have been studied. Normally, CdSe exists in two crystalline forms: stable hexagonal (wurtzite) phase and the metastable cubic (sphalerite) phase. The CdSe thin films prepared by electrodeposition are normally found to be either in the metastable cubic phase or as a mixture of cubic and hexagonal phases. Transition from metastable cubic to stable hexagonal phase in CdSe thin films by thermal annealing has also been reported in literature.[26] But to the best of our knowledge, no work has been reported on swift heavy Ag^{9+} ion (120 Mev) irradiation induced structural phase transformation in electrodeposited CdSe thin film of thickness 110 nm. The present work reports the SHI induced phase transformation and hence modification in the structural, morphological and luminescence properties of CdSe thin film. The present study may prove to be beneficial for the utilization of semiconducting nanostructures in the future nanoscale devices and opens up new avenues for research to modulate opto-electronic properties of CdSe thin films for the better device applications.

2. EXPERIMENTAL PROCEDURE

2.1 Synthesis of CdSe thin films

Thin films of cadmium selenide (CdSe) were electro-deposited potentiostatically on indium tin oxide (ITO) coated glass substrates. The electro-deposition was done by using SP-240 potentiostat employing a conventional three electrode set-up. The electrochemical cell consisted of Ag/AgCl electrode as the reference electrode; an indium tin oxide (ITO) coated glass substrates with sheet resistance of 10 ohms/sq as the working electrode and platinum wire (length-5.7 cm, diameter-0.5 mm) as the counter electrode. For the deposition, aqueous solutions containing 0.2 M $3CdSO_4 \cdot 8H_2O$ and 0.25 mM SeO_2 were used. The electrolyte was constantly stirred by using Teflon coated magnetic paddle to dissolve the precursors completely in de-ionized water. The pH of the electrolyte was adjusted between 2 and

3 by using concentrated H_2SO_4. The total volume of electrolyte taken was 50 mL at room temperature. Before deposition, the ITO substrates were ultrasonically cleaned with distilled water and acetone successively. For electro deposition, the potential was set at −0.75 V and time of deposition was 10 minutes. After deposition, the CdSe thin film on ITO substrate was taken out from the electrolyte and rinsed with de-ionized water to remove loosely bound precipitates. The sample was thereafter dried in air at 100 °C for 15 minutes. Thickness of the deposited CdSe thin film obtained was 110 nm, estimated using stylus profilometer.

2.2 Growth kinetics

Deposition of CdSe thin film occurs when the ionic product of Cd^{2+} and Se^{2+} ions exceeds the solubility product of CdSe. Growth mechanism of CdSe thin film on ITO substrate may be understood with chemical reactions as follows,

$$3CdSO_4 \cdot 8H_2O + H_2O \longrightarrow 3Cd^{2+} + 3SO_4^{2-} + 9H_2O$$
$$SeO_2 + H_2O \longrightarrow H_2SeO_3$$

On reduction of H_2SeO_3,

$$H_2SeO_3 + 4H^+ + 6e^- \longrightarrow Se^{2-} + 3H_2O$$

And formation of CdSe takes place according to chemical reaction[27]

$$Cd^{2+} + Se^{2-} \longrightarrow CdSe$$

2.3 Swift heavy ions irradiation

The as-deposited thin films of CdSe were irradiated with 120 MeV, Ag^{9+} ions using 15 UD Pelletron accelerators at IUAC, New Delhi, India. The films were irradiated in a high vacuum (~10^{-6} mbar) chamber at normal incidence to the sample surface. The ion beam was raster scanned by a magnetic scanner on the sample surface to maintain the constant ion flux throughout the sample surface. The area of irradiated thin film sample was 1 cm^2. The samples were irradiated at different fluences of 3×10^{11}, 3×10^{12} and 3×10^{13} ions/cm^2. The energy regime for SHI irradiation was selected after simulation using Stopping and Range of Ions in Matter (SRIM) code. For the chosen ion energy of 120 MeV, the lateral straggling was 1.27 μm and longitudinal straggling was 0.99 μm with penetration depth 13.43 μm. This value of penetration depth was greater than the thickness (110 nm) of the CdSe thin film. The energy of the Ag^{9+} beams (120 MeV) was selected with a view to avoid ion implantation in CdSe thin films.

2.4 Characterization

The morphological, structural, and electrical properties of pristine and irradiated thin films were characterized by using a scanning electron microscope (JEOL/EO JSM-6390), X-ray diffractometer (Rigaku MiniFlexII) and four probe set up employing with it, a programmable current and voltage source meter (Keithley-2400) respectively. XRD spectra were recorded using CuK_α radiation (λ = 1.5406 Å) at 30 kV and 15 mA with a scanning rate of 2 min^{-1} for 2θ values ranging from 20 ° to 80 °. For studying optical properties, absorption spectra were recorded using UV-visible double beam 550 Spectrophotometer (Camspec) in the spectral range 200-900 nm at room temperature. Photoluminescence analysis of prepared samples was carried out on SHIMADZU, a RF-530 Spectro fluorophotometer in the range 200-900 nm. The surface roughness of the films was measured using Atomic Force Microscope (AFM) while the chemical composition of the films was analyzed using the standard energy dispersive analysis of X-ray (EDX).

3. RESULTS AND DISCUSSION

3.1 Structural analysis

X-ray diffraction pattern of as-deposited and Ag^{9+} ions irradiated CdSe thin films exposed to different fluences (3×10^{11} to 3×10^{13} ions/cm^2) are shown in Fig. 1. XRD pattern revealed that as-deposited CdSe thin films are of polycrystalline nature and are found to have mixed phase of CdSe (both cubic and hexagonal). Peaks were indexed to JCPDS cards 65-2891 and 77-2307 for cubic CdSe and hexagonal CdSe. Apart from mixed phases of CdSe thin film obtained, a separate peak at 2θ = 38.3 ° (JCPDS files no. 02-0677) was also observed corresponding to selenium. During irradiation with swift heavy Ag^{9+} ions, two competing processes occured simultaneously; (1) the generation of vacancies, agglomeration of vacancies and then collapsing into dislocation loops (2) their annihilation at possible sinks with increasing ions fluences.[28]

Hence, after Ag^{9+} ions irradiation, observed XRD pattern showed that the metastable cubic phase gets transformed into a stable hexagonal phase with the changing ion fluence. The peak at 2θ = 61.2 ° that was exclusively due to cubic phase of CdSe decreased with increasing fluences and disappeared completely at of fluence 3×10^{13} ions/cm^2 and simultaneously a new peak at 2θ = 64 ° corresponding to hexagonal phase appeared after irrariation in the XRD pattern of CdSe thin film. These observations suggest that mixed phase have transformed to a stable hexagonal phase due to irradiation induced annealing. A number of investigators have reported similar transition from cubic to hexagonal phase on annealing.[29-31] The intensity of Se peak at 2θ = 38.3 ° was found to increase with fluence due to increase in temperature during irradiation. Similar effect has also been reported.[32] The grain size was calculated using Debye-Scherrer's formula,[33]

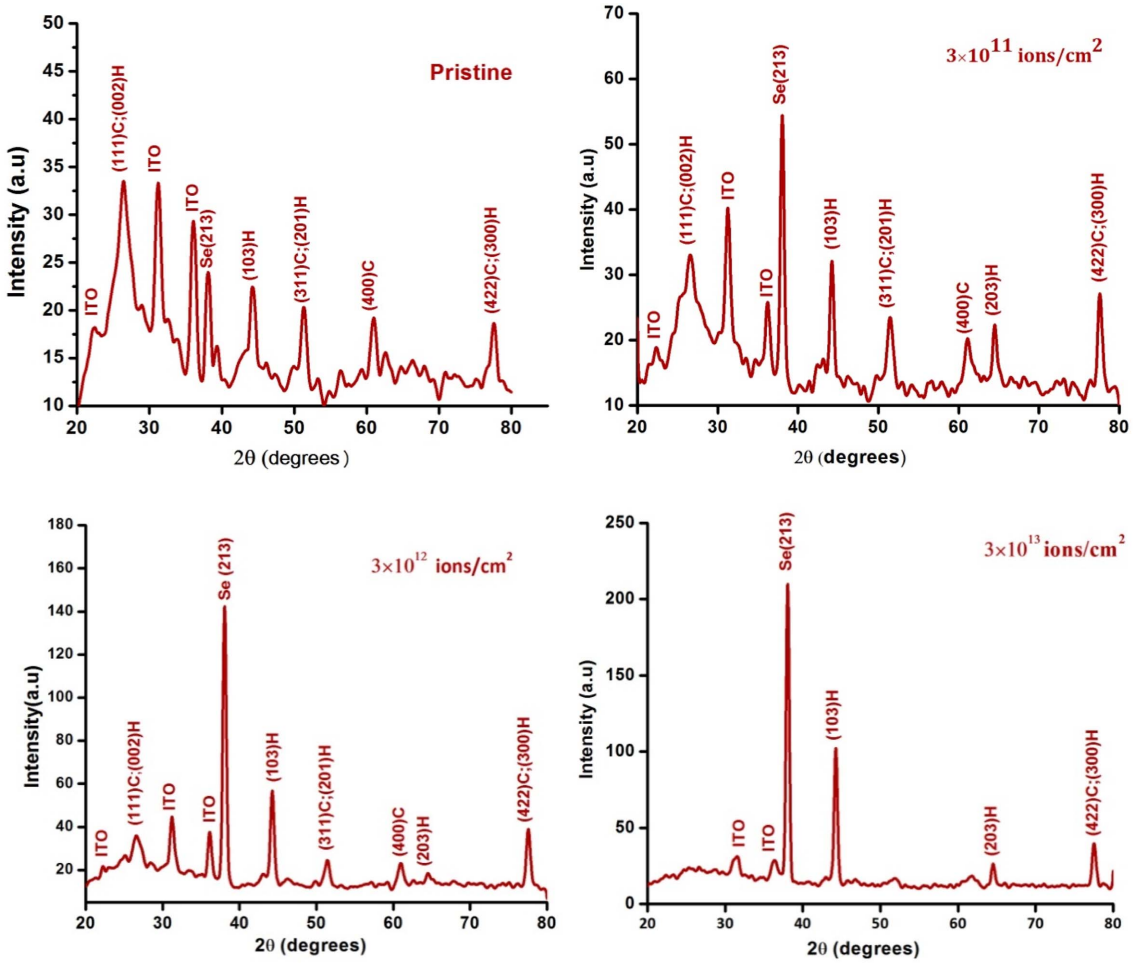

Fig. 1. The XRD patterns of pristine and Ag^{9+} ions irradiated CdSe thin films at fluencies 3×10^{11}, 3×10^{12} and 3×10^{13} ions/cm^2.

Table 1. Structural parameters of pristine and irradiated CdSe thin film at different fluences.

Fluence (ions/cm$^{2)}$	FWHM of (213) (deg)	FWHM of (103) (deg)	FWHM of (422)C;(300)H (deg)	Av. Grain Size D (nm)	Av. Micro Strain (10^{-3} lin^{-2}m^{-4})
Pristine	0.836	0.774	0.877	10.14	4.21
3×10^{11}	0.551	0.547	0.673	12.21	4.19
3×10^{12}	0.507	0.564	0.601	14.14	2.79
3×10^{13}	0.456	0.502	0.587	19.76	1.85

$$D = (0.9\lambda)/(\beta\cos\theta)$$

where D is mean grain (crystallite) size, β is full width at half maxima (FWHM) of the peak intensity, θ is the diffraction angle and λ is the wavelength of X-ray radiation.The calculated grain size was found to increase from 10.14 nm to 19.76 nm with increase in ion fluence as listed in Table 1. The possible structural modification by irradiation may be due to the energy deposition in the films by energetic Ag^{9+} ions. The imparted energy of incoming ions to the host sample release the strain energy in the films and results in further improvement of the crystalline quality of CdSe thin film. Similar results have been reported in literature for ZnO thin films and also for bare and coated ZnS quantum dots by SHI irradiation.[34,35] The summary of XRD data and calculated structural parameters of pristine and irradiated CdSe thin films with different fluences are presented in Table 1. The variation of FWHM of different planes with increase in ion fluence is shown in Fig. 2.

The micro strain (ε) in the thin film is the disarrangement

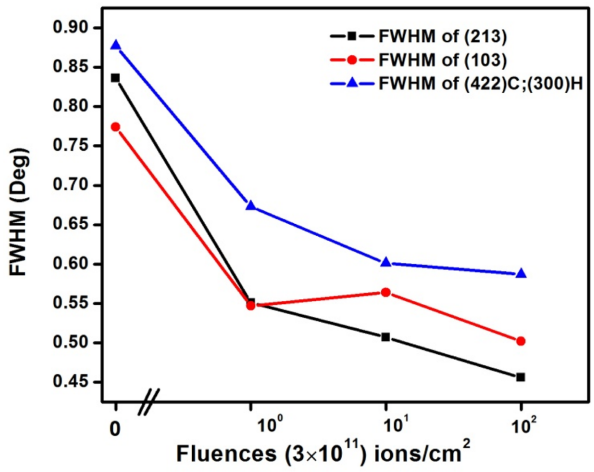

Fig. 2. Variation of FWHM of different planes with Ag^{9+} ions fluencies ; 3×10^{11}, 3×10^{12} and 3×10^{13} ions/cm^2.

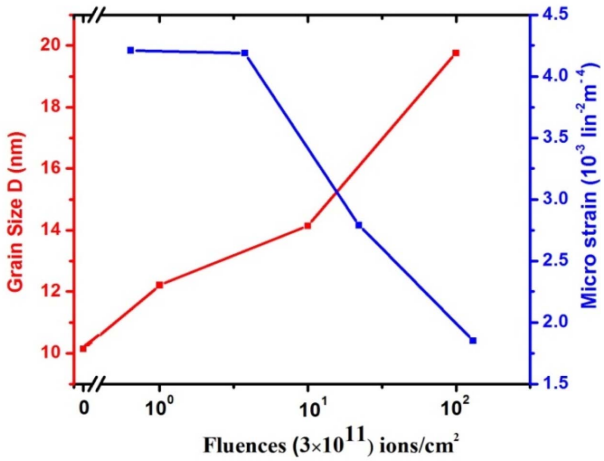

Fig. 3. Variation of average grain size and micro strain with Ag^{9+} ions fluences at 3×10^{11}, 3×10^{12} and 3×10^{13} ions/cm^2.

of lattice created during deposition process and is calculated by using the relation,[33]

$$\varepsilon = (\beta\cos\theta)/4$$

The strain decreased from 4.21 to 1.85 with ion fluence as listed in Table 1. It may be attributed to the lattice vibrations that are induced by the incident ion energy in single tracks which may help in the reorientation of some regions and hence minimize the interfacial energy between grains.[34] The variation of grain size and micro strain with ion fluence is shown in Fig. 3.

3.2 Morphological and compositional analysis

Surface morphology of as-deposited and SHI irradiated CdSe thin films were investigated by using SEM (Fig. 4). SEM images of irradiated samples revealed that the smoothness and uniformity of thin films increased upto fluence 3×10^{12} ions/cm^2. When the fluence was further increased to 3×10^{13} ions/cm^2, coalescence between grains may have occurred due to rise in temperature. The composition of pristine CdSe thin film was analyzed using EDX (Fig. 5). The average weight percentage of Cd: Se is found to be 34:66, which shows the Se rich CdSe thin film

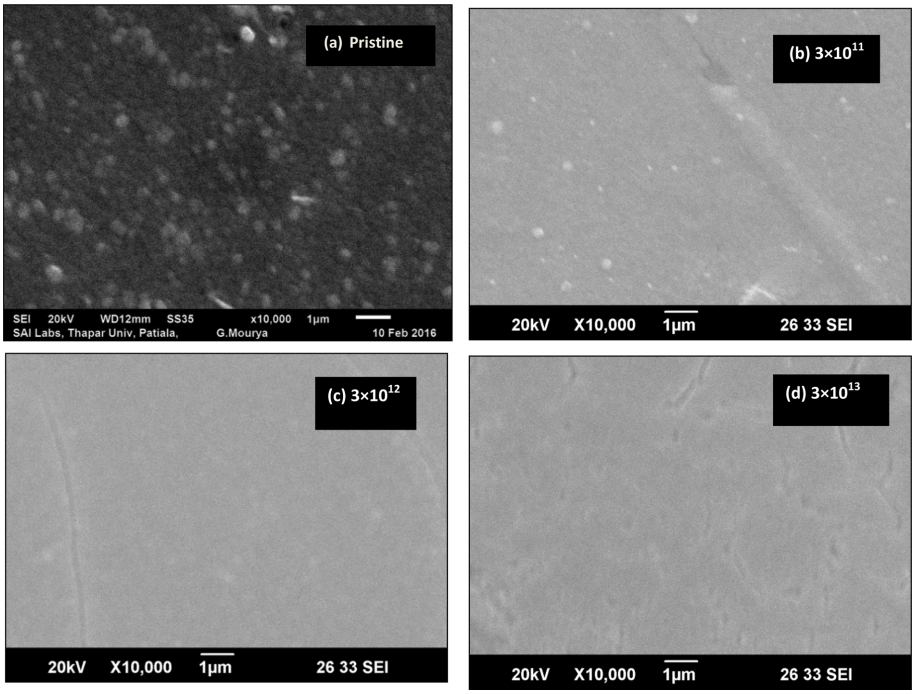

Fig. 4. SEM images of (a) pristine CdSe thin film (b) Ag^{9+} ion irradiated CdSe thin film with fluences 3×10^{11}, (c) 3×10^{12} and (d) 3×10^{13} ions/cm^2.

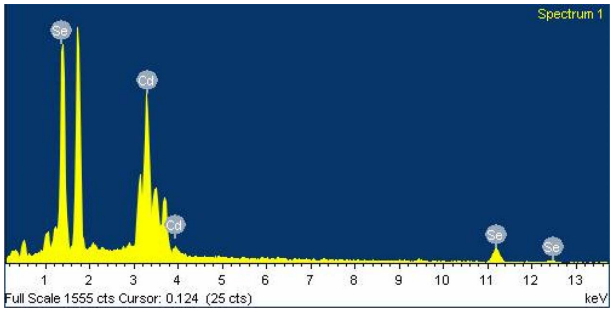

Fig. 5. EDX analysis of pristine CdSe thin film.

due to highly reactive nature of Se ions as compared to Cd ions (also confirmed by XRD due to separate formation of Se plane). Rest of the peaks in EDX is due to ITO coated glass substrate.

Element	Weight (%)
Se L	66.24
Cd L	33.76

The surface morphology of pristine and irradiated CdSe thin films was also studied using AFM (Fig. 6). Information from AFM images is usually quantified in terms of average roughness (R_a) and rms roughness (R_q). R_a represents mean value of the surface height with respect to a centre plane whereas R_q is the standard deviation of the surface height within the given area.

The 2D AFM images of as deposited film has cubical grain shapes. Under the effect of irradiation, the surface roughness was found to decrease as the fluence increases from 3×10^{11} to 3×10^{12} ions/cm^2. The decrease in surface roughness with ion fluence suggests the existence of a surface smoothening process. When the fluence is further increased to 3×10^{13} ions/cm^2, an increase in surface roughness is observed (Table 2), which is in good agreement with SEM results. The observed smoothening of the surface with initial fluence and subsequent roughening at higher fluences was explained on the basis of positive heat mixing of the elements which prevents inter- diffusion across the interface during the thermal spike.

For the film irradiated at a fluence of 3×10^{11} and 3×10^{12} ions/cm^2, the dominant surface transport mechanism is

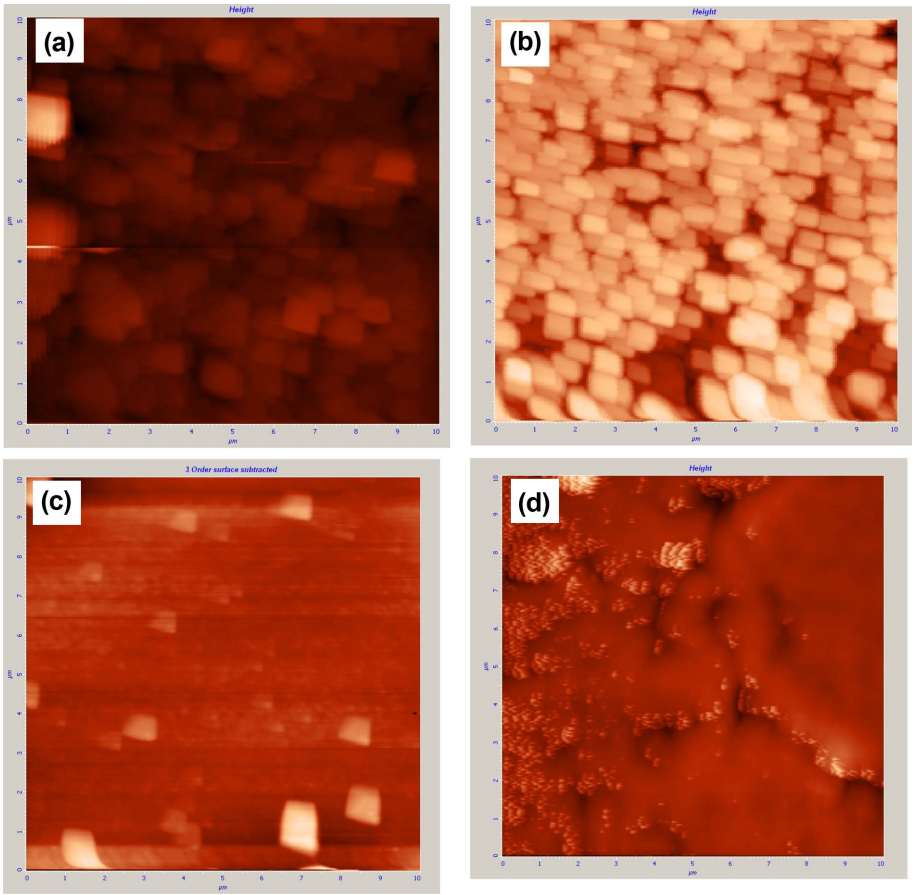

Fig. 6. AFM images of (a) as-deposited CdSe thin film (b) irradiated with Ag^{9+} ion fluence 3×10^{11} ions/cm^2 (c) 3×10^{12} ions/cm^2 and (d) 3×10^{13} ion/cm^2.

Table 2. Surface roughness of pristine and Ag^{9+} irradiated CdSe thin film with different fluence.

Fluence (ions/cm^2)	R.M.S roughness, R_q (nm)	Avg. roughness, R_a (nm)
Pristine	38.1	26.0
3×10^{11}	32.4	24.7
3×10^{12}	17.6	10.7
3×10^{13}	27.8	18.9

evaporation-condensation which explains the surface smoothening observed at these fluences. However, as the fluence was increased to 3×10^{13} ions/cm^2, the dominant mechanism becomes volume diffusion. Thus the roughening was observed in the films at high fluences due to thermal spike. Similar effects also observed in Ag^{+7} ion irradiated Co-Fe-Si thin films.[36]

3.3 Optical analysis

The optical properties of the as deposited and irradiated CdSe thin films were examined by UV-visible double beam 550 Spectrophotometer (Camspec) in the spectral range 200-900 nm at room temperature. The optical energy band gap (E_g) of as-deposited and Ag^{9+} ion irradiated CdSe thin film was determined with the help of well-known relation of Tauc,[37]

$$\alpha h\nu = A\,(h\nu - E_g)^m$$

where 'A' is a constant, 'α' is absorption coefficient and value of 'm' decides the type of transition. Value of 'm' is 1/2, 2, 3 and 3/2 for direct allowed, indirect allowed, indirect forbidden and direct forbidden transitions respectively. The present system obeys the rule of direct transition i.e. m = ½. The bandgap of pristine and irradiated samples is determined using Tauc's plot of $(\alpha h\nu)^2$ versus (hν) (Fig. 7).

The bandgap of CdSe thin films decreased in steps of 2.47 eV, 2.37 eV, 2.29 eV and 2.12 eV with increasing ion fluence 3×10^{11} ions/cm^2 (Ag-1), 3×10^{12} ions/cm^2 (Ag-2) and 3×10^{13} ions/cm^2 (Ag-3). The high energy irradiation induced lattice damage creates defect energy levels below the conduction band and hence band gap decreases.[38] Also, the lattice damage is proportional to irradiation fluence and hence due to the band tailing effect band gap decreases continuously with increase in ion fluence.[39]

Photoluminescence (PL) spectra of as-deposited and irradiated CdSe thin films were obtained from SHIMADZU, a RF-530 Spectro fluorophotometer in the range 350-650 nm. A typical PL spectrum is a sensitive and powerful technique for the study of defects in thin films. The PL spectrum of as-deposited CdSe thin film shows a strong emission band centered at 606 nm (Fig. 8). The excitation wavelength taken was 400 nm. The PL Intensity is directly related to defect concentrations as the concentration of

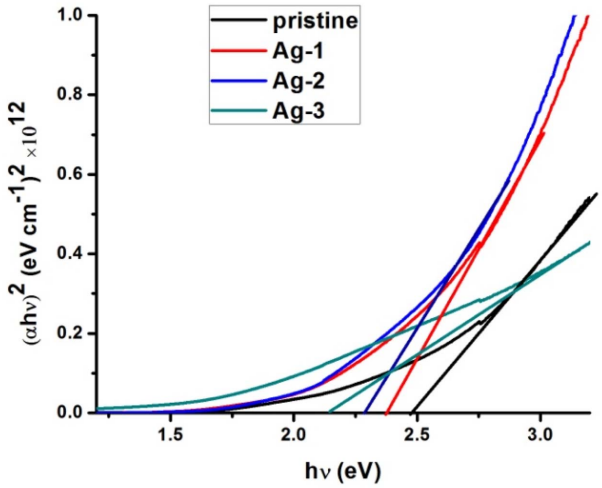

Fig. 7. The tauc-plot of pristine and Ag^{9+} ion irradiated CdSe thin film with fluence, Ag-1 (3×10^{11}), Ag-2 (3×10^{12}) and Ag-3 (3×10^{13}).

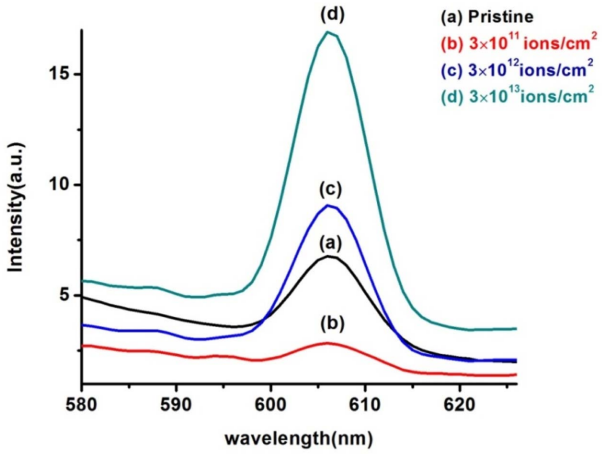

Fig. 8. PL spectrum of (a) as-deposited, and irradiated CdSe thin film with Ag^{9+} ion of fluence (b) 3×10^{11}, (c) 3×10^{12} and (d) 3×10^{13} ions/cm^2.

defects is increases at higher fluencies, the PL intensity also increases. In our case, at low Ag^{9+} ions fluence 3×10^{11} ions/cm^2, the formation of exciton take place which may be trapped by the defects. Hence, when CdSe thin film was initially irradiated with Ag^{9+} ions fluence 3×10^{11} ions/cm^2, the PL peak intensity decreases compare to pristine case. Similar results for 40 MeV Li^{3+} ions irradiated Tris-(8-hydroxyquinoline) aluminum (Alq_3) thin films were also reported.[40] When CdSe thin film was further irradiated with higher Ag^{9+} ion fluence from 3×10^{12} to 3×10^{13} ions/cm^2, an increase in the PL peak intensity was observed (Fig. 8). The increasing trend observed in PL intensity might be due to increase in defect concentration caused by Ag^{9+} ion irradiation.[41] The shift of peak towards higher wavelength

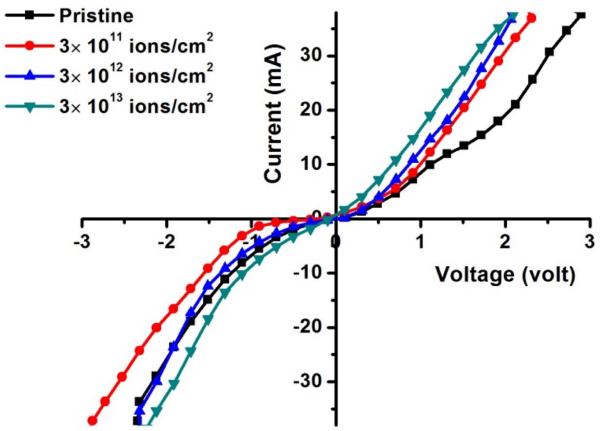

Fig. 9. The current-voltage characteristics of as-deposited and Ag^{9+} ion irradiated CdSe thin film with different fluences.

Table 3. The electrical resistivity of pristine and irradiated Ag^{9+} ion CdSe thin films.

S. No.	Ion fluence (ions/cm^2)	Electrical resistivity (Ω-cm)
1.	Pristine	28.26
2.	Ag-1 (3×10^{11})	25.12
3.	Ag-2 (3×10^{12})	21.35
4.	Ag-3 (3×10^{13})	20.34

side (about 0.2 nm) also shows decrease in the optical band gap with fluence, which is in good agreement with the Tauc-plot.

3.4 Electrical analysis

The current-voltage characteristics of as-deposited and Ag^{9+} ion irradiated CdSe thin film by four probe method are shown in Fig. 9. The electrical resistivity (ρ) of thin film was calculated using relation,[42]

$$\rho = 2\pi s\,(V/I)$$

where 's' is the distance between probes and having value 1 mm. The calculated values of resistivity for as-deposited and irradiated CdSe thin films are listed in Table 3.

The observed I-V characteristic at all fluences suggests the semiconducting nature of CdSe thin films. Electrical resistivity calculated, was found to decrease with increase in fluence. The increase in grain size from 10.14 nm to 19.76 nm with ion fluence in thin films may result with significant resistivity decrease due to reduction in grain boundary scattering.[43]

4. CONCLUSIONS

Following conclusions can be drawn from the present investigations:

1. CdSe thin films of thickness 110 nm were electro-deposited on ITO glass substrate and subsequently irradiated with 120 MeV Ag^{9+} SHI at fluencies ranging from 3×10^{11} to 3×10^{13} ions/cm^2.
2. XRD analysis confirmed the structural phase trans-formation from mixed phase to stable hexagonal phase with increase in crystallinity.
3. The phenomenon of phase transformation may be attributed to the creation of high pressure and temperature by thermal spike during passage of 120 MeV Ag^{9+} ion beam through CdSe thin film.
4. The AFM and SEM studies revealed decrease in film roughness upto fluence 3×10^{12} ions/cm^2 and thereafter the roughness increased at higher fluences due to thermal spike.
5. The optical band gap of the samples was found to decrease from 2.47 to 2.12 eV with fluence due to the structural transformations.
6. Photoluminescence analysis revealed an improvement in optical characteristics due increase in concentration of defects at high ion fluencies.

The Structural analysis confirmed the phase transformation from mixed phase to hexagonal phase due to thermal spike resulting in increase of roughness as indicated by SEM/ AFM images. Due to structural transformation decrease in band gap was observed resulting decrease in resistivity as revealed by electrical properties. Hence, we conclude that changes in properties are correlated with each other.

ACKNOWLEDGEMENTS

The authors like to thank the Director and the technical staff of pelletron group for their help during the irradiation experiment at Inter University Accelerator Centre (IUAC), New Delhi, India. Authors also acknowledge NIT Kurukshetra, India for providing SEM, XRD, AFM, UV-Spectrophotometer and PL-Spectrophotometer facilities and SAI Lab, Thapar University, Patiala, India for providing EDX facility.

REFERENCES

1. Y. P. Gnatenko, P. M. Bukivskij, A. S. Opanasyuk, D. I. Kurbatov, M. M. Kolesnyk, V. V. Kosyak, and H. Khlyap, *J. Lumin.* **132**, 2885 (2012).
2. S. Thanikaikarasan, X. S. Shajan, V. Dhanasekaran, and T. Mahalingam, *J. Mater. Sci.* **46**, 4034 (2011).
3. P. K. Nair, M. T. S. Nair, V. M. Garcia, O. L. Arenas, Y. Pena, A. Castillo, I. T. Ayala, O. Gomezdaza, A. Sanchez, J. Campos, H. Hu, R. Suarez, and M. E. Rincon, *Sol. Energ. Mat. Sol. C.* **52**, 313 (1998).
4. D. H. Lee, J. M. Kim, K.-T. Lim, H. J. Cho, J. H. Bang, and Y. S. Kim, *Electron. Mater. Lett.* **12**, 276 (2016).
5. A. V. Calster, A. Vervaet, I. D. Rycke, J. D. Baets, and J. Vanfleteren, *J. Cryst. Growth* **86**, 924 (1989).

6. Y. P. Gnatenko, P. M. Bukivskij, I. O. Faryna, A. S. Opanasyuk, and M. Ivashchenko, *J. Lumin.* **146**, 174 (2014).
7. M. H. Yükselici, A. A. Bozkurt, and B. C. Ömür, *Mater. Res. Bull.* **48**, 2442 (2013).
8. C. Baban and G. I. Rusu, *Appl. Surf. Sci.* **211**, 6 (2003).
9. S. Devadason and M. R. Muhamad, *Physica B* **393**, 125 (2007).
10. P. P. Hankare, P. A. Chate, D. J. Sathe, M. R. Asabe, and B. V. Jadha, *J. Alloy Compd.* **474**, 347 (2009).
11. Y. Yan, F. Jiang, L. Liu, Z. Yu, Y. Zhang, and Y. Zhao, *Electron. Mater. Lett.* **12**, 59 (2016).
12. R. I. Chowdhury, M. S. Islam, F. Sabeth, G. Mustafa, S. F. U. Farhad, D. K. Saha, F. A. Chowdhury, S. Hussain, and A. B. M. O. Islam, *Dhaka Univ. J. Sci.* **60**, 137 (2012).
13. S. K. Shinde, D. P. Dubal, G. S. Ghodake, D. S. Lee, G. M. Lohar, M. C. Rath, and V. J. Fulari, *Mater. Lett.* **132**, 243 (2014).
14. S. M. Rashwan, S. M. Abd El-Wahab, and M. M. Mohamed, *J. Mater. Sci.: Mater. El.* **18**, 575 (2007).
15. D. C. Agarwal, A. Kumar, S. A. Khan, D. Kabiraj, F. Singh, A. Tripathi, J. C. Pivin, R. S. Chauhan, and D. K. Avasthi. *Nucl. Instrum. Meth. B* **244**, 136 (2006).
16. V. Kumar, F. Singh, O. M. Ntwaeaborwa, and H. C. Swart, *Appl. Surf. Sci.* **279**, 472 (2013).
17. D. Kanjilal, *Curr. Sci. India* **80**, 1560 (2001).
18. V. V. Ison, A. R. Rao, V. Dutta, P. K. Kulriya, D. K. Avasthi, and S. K. Tripathi, *J. Appl. Phys.* **106**, 023508 (2009).
19. V. V. Ison, A. R. Rao, V. Dutta, P. K. Kulriya, and D. K. Avasthi, *Nucl. Instrum. Meth. B* **267**, 2480 (2009).
20. P. Stampfli, *Nucl. Instrum. Meth. B* **107**, 138 (1996).
21. H. P. Cheng and J. D. Gillaspy, *Phys. Rev. B* **55**, 2628 (1997).
22. M. Toulemonde, C. Dufour, and E. Paumier, *Phys. Rev. B* **46**, 14362 (1992).
23. W. Wesch, A. Kamarou, and E. Wendler, *Nucl. Instrum. Meth. B* **225**, 111 (2004).
24. A. Berthelot, S. Hemon, F. Gourbilleau, C. Dufour, E. Dooryhee, and E. Paumier, *Nucl. Instrum. Meth. B* **146**, 437 (1998).
25. S. P. Patel, A. K. Chawla, R. Chandra, J. Prakash, P. K. Kulriya, J. C. Pivin, D. Kanjilal, and L. Kumar, *Solid State Commun.* **150**, 1158 (2010).
26. S. Erat, H. Metin, and M. Ari, *Mater. Chem. Phys.* **111**, 114 (2008).
27. T. Mahalingam, R. Mariappan, V. Dhanasekaran, S. M. Mohan, G. Ravi, and J. P. Chu, *Chalcogenide Lett.* **7**, 669 (2010).
28. R. Sivakumar, C. Sanjeeviraja, M. Jayachandran, R. Gopalakrishnan, S. N. Sarangi, D. Paramanik, and T. Som, *J. Phys. D: Appl. Phys.* **41**, 125304 (2008).
29. O. Z. Angel, J. J. Alvarado-Gil, R. L. Morales, and H. Vargas, *Appl. Phys. Lett.* **64**, 291 (1994).
30. O. Z. Angel, L. Hernandez, O. D. Melo, J. J. Alvarado-Gil, R. L. Morales, C. Falcony, H. Vargas, and R. R. Bon, *Vacuum* **46**, 1083 (1995).
31. K. L. Narayanan, K. P. Vijayakumar, K. G. M. Nair, N. S. Thampi, and K. Krishan, *J. Mater. Sci.* **32**, 4837 (1997).
32. H. M. Kotb, M. A. Dabban, A. Y. A. Latif, and M. M. Hafiz, *J. Alloy Compd.* **512**, 115 (2012).
33. S. Shanmugan and D. Mutharasu, *Radiat. Phys. Chem.* **81**, 201 (2012).
34. D. C. Agarwal, D. K. Avasthi, F. Singh, D. Kabiraj, P. K. Kulariya, I. Sulania, J. C. Pivin, and R. S. Chauhan, *Surf. Coat. Tech.* **203**, 2427 (2009).
35. S. Chowdhury, A. M. P. Hussain, G. A. Ahmed, F. Singh, D. K. Avasthi, and A. Choudhury, *Mater. Res. Bull*. **43**, 3495 (2008).
36. T. Hysen, P. Geetha, S. A. Harthi, I. A. Al-Omari, R. Lisha, R. V. Ramanujan, D. Sakthikumar, D. K. Avasthi, and M. R. Anantharaman, *J. Magn. Magn. Mater.* **372**, 224 (2014).
37. J. Tauc, *New York: Plenum Press* **171**, 159 (1974).
38. S. Soundeswaran, O. S. Kumar, P. Ramasamy, D. K. Raj, D. K. Avasthi, and R. Dhanasekaran, *Physica B* **355**, 222 (2005).
39. R. Sivakumar, C. Sanjeeviraja, M. Jayachandran, R. Gopalakrishnan, S. N. Sarangi, D. Paramanik, and T. Som, *J. Appl. Phys*. **101**, 034913 (2007).
40. K. Thangaraju, R. Kumaran, K. Asokan, P. Ramamoorthy, D. Kanjilal, and J. Kumar, *Surf. Coat. Tech*. **203**, 2679 (2009).
41. N. Manikanthababu, M. Dhanunjaya, S. V. S. N. Rao, and A. P. Pathak, *Nucl. Instrum. Meth. B* 2016 (in press).
42. A. Purohit, S. Chander, S. P. Nehra, and M. S. Dhaka, *Physica E* **69**, 342 (2015).
43. P. M. R. Kumar, C. S. Kartha, K. P. Vijayakumar, F. Singh, D. K. Avasthi, T. Abe, Y. Kashiwabe, G. S. Okram, M. Kumar, and S. Kumar, *J. Appl. Phys.* **97**, 013509 (2005).